

## 4.4. SCATTERING FROM MESOMORPHIC STRUCTURES

The amplitude  $\sigma \propto t^{-\gamma}$ , where the measured values of  $\gamma$  are empirically found to be very close to the measured values for the sum  $\nu_{\parallel} + \nu_{\perp}$ . Most of the systems that have been measured to date have values for  $\nu_{\parallel} > 0.66 > \nu_{\perp}$  and  $\nu_{\parallel} - \nu_{\perp} \approx 0.1$  to 0.2. Table 4.4.2.1 lists sources of the observed values for  $\gamma$ ,  $\nu_{\parallel}$  and  $\nu_{\perp}$ . The theoretical and experimental studies of this pretransition effect account for a sizeable fraction of all of the liquid-crystal research in the last 15 or 20 years, and as of this writing the explanation for these two different temperature dependences remains one of the major unresolved theoretical questions in equilibrium statistical physics.

It is very likely that the origin of the problem is the QLRO in the position of the smectic layers. Lubensky attempted to deal with this by introducing a gauge transformation in such a way that the thermal fluctuations of the transformed order parameter did not have the logarithmic divergence. While this approach has been informative, it has not yet yielded an agreed-upon understanding. Experimentally, the effect of the phase can be studied in systems where there are two competing order parameters with wavevectors that are at  $\mathbf{q}_2$  and  $\mathbf{q}_1 \approx 2\mathbf{q}_2$  (Sigaud *et al.*, 1979; Hardouin *et al.*, 1983; Prost & Barois, 1983; Wang & Lubensky, 1984; Chan, Pershan *et al.*, 1985). On cooling, mixtures of 4-hexylphenyl 4-(4-cyanobenzoyloxy)benzoate (DB<sub>6</sub>) and *N,N'*-(1,4-phenylenedimethylene)bis(4-butylaniline) (also known as terephthal-bis-butylaniline, TBBA) first undergo a second-order transition from the nematic to a phase that is designated as smectic-A<sub>1</sub>. The various smectic-A and smectic-C morphologies will be described in more detail in the following section; however, the smectic-A<sub>1</sub> phase is characterized by a single peak at  $q_1 = 2\pi/d$  owing to a one-dimensional density wave with wavelength  $d$  of the order of the molecular length  $L$ . In addition, however, there are thermal fluctuations of a second-order parameter with a period of  $2L$  that give rise to a diffuse peak at  $q_2 = \pi/L$ . On further cooling, this system undergoes a second second-order transition to a smectic-A<sub>2</sub> phase with QLRO at  $q_2 \approx \pi/L$ , with a second harmonic that is exactly at  $q = 2q_2 \approx 2\pi/L$ . The critical scattering on approaching this transition is similar to that of the nematic to smectic-A<sub>1</sub>, except that the pre-existing density wave at  $q_1 = 2\pi/L$  quenches the phase fluctuations of the order parameter at the subharmonic  $q_2 = \pi/L$ . The measured values of  $\nu_{\parallel} = \nu_{\perp} \approx 0.74$  (Chan, Pershan *et al.*, 1985) agree with those expected from the appropriate theory (Huse, 1985). A mean-field theory that describes this effect is discussed in Section 4.4.3.2 below.

It is interesting to note that even those systems for which the nematic to smectic-A transition is first order show some pretransitional lengthening of the correlation lengths  $\xi_{\parallel}$  and  $\xi_{\perp}$ . In these cases, the apparent  $T^*$  at which the correlation lengths would diverge is lower than  $T_{\text{NA}}$  and the divergence is truncated by the first-order transition (Ocko *et al.*, 1984).

## 4.4.3. Smectic-A and smectic-C phases

## 4.4.3.1. Homogeneous smectic-A and smectic-C phases

In the smectic-A and smectic-C phases, the molecules organize themselves into layers, and from a naive point of view one might describe them as forming a one-dimensional periodic lattice in which the individual layers are two-dimensional liquids. In the smectic-A phase, the average molecular axis  $\langle \mathbf{n} \rangle$  is normal to the smectic layers while for the smectic-C it makes a finite angle. It follows from this that the smectic-C phase has lower symmetry than the smectic-A, and the phase transition from the smectic-A to smectic-C can be considered as the ordering of a two-component order parameter, *i.e.* the two components of the projection of the molecular axis on the smectic layers (De Gennes, 1973). Alternatively, Chen & Lubensky (1976) have developed a mean-field theory in which the transition is described by a free-energy density of the Lifshitz form. This will

Table 4.4.2.1. Summary of critical exponents from X-ray scattering studies of the nematic to smectic-A phase transition

Molecule	$\gamma$	$\nu_{\parallel}$	$\nu_{\perp}$	Reference
4O.7	1.46	0.78	0.65	(a)
8S5	1.53	0.83	0.68	(b), (g)
CBOOA	1.30	0.70	0.62	(c), (d)
4O.8	1.31	0.70	0.57	(e)
8OCB	1.32	0.71	0.58	(d), (f)
9S5	1.31	0.71	0.57	(b), (g)
8CB	1.26	0.67	0.51	(h), (i)
10S5	1.10	0.61	0.51	(b), (g)
9CB	1.10	0.57	0.39	(g), (j)

References: (a) Garland *et al.* (1983); (b) Brisbin *et al.* (1979); (c) Djurek *et al.* (1974); (d) Litster *et al.* (1979); (e) Birgeneau *et al.* (1981); (f) Kasting *et al.* (1980); (g) Ocko *et al.* (1984); (h) Thoen *et al.* (1982); (i) Davidov *et al.* (1979); (j) Thoen *et al.* (1984).

be described in more detail below; however, it corresponds to replacing equation (4.4.2.5) for the free energy  $\Delta F(\psi)$  by an expression for which the minimum is obtained when the wave-vector  $\mathbf{q}$ , of the order parameter  $\psi \propto \exp[i\mathbf{q} \cdot \mathbf{r}]$ , tilts away from the molecular axis.

The X-ray cross section for the prototypical aligned monodomain smectic-A sample is shown in Fig. 4.4.1.2(b). It consists of a single sharp spot along the molecular axis at  $|\mathbf{q}|$  somewhere between  $2\pi/2L$  and  $2\pi/L$  that reflects the QLRO along the layer normal, and a diffuse ring in the perpendicular direction at  $|\mathbf{q}| \approx 2\pi/a$  that reflects the SRO within the layer. The scattering cross section for an aligned smectic-C phase is similar to that of the smectic-A except that the molecular tilt alters the intensity distribution of the diffuse ring. This is illustrated in Fig. 4.4.1.2(c) for a monodomain sample. Fig. 4.4.1.2(d) illustrates the scattering pattern for a polydomain smectic-C sample in which the molecular axis remains fixed, but where the smectic layers are randomly distributed azimuthally around the molecular axis.

The naivety of describing these as periodic stacks of two-dimensional liquids derives from the fact that the sharp spot along the molecular axis has a distinct temperature-dependent shape indicative of QLRO that distinguishes it from the Bragg peaks due to true LRO in conventional three-dimensional crystals. Landau and Peierls discussed this effect for the case of two-dimensional crystals (Landau, 1965; Peierls, 1934) and Caillé (1972) extended the argument to the mesomorphic systems.

The usual treatment of thermal vibrations in three-dimensional crystals estimates the Debye–Waller factor by integrating the thermal expectation value for the mean-square amplitude over reciprocal space (Kittel, 1963):

$$W \simeq \frac{k_{\text{B}}T}{c^3} \int_0^{k_{\text{D}}} \frac{k^{(d-1)}}{k^2} dk, \quad (4.4.3.1)$$

where  $c$  is the sound velocity,  $\omega_{\text{D}} \equiv ck_{\text{D}}$  is the Debye frequency and  $d = 3$  for three-dimensional crystals. In this case, the integral converges and the only effect is to reduce the integrated intensity of the Bragg peak by a factor proportional to  $\exp(-2W)$ . For two-dimensional crystals  $d = 1$ , and the integral, of the form of  $dk/k$ , obtains a logarithmic divergence at the lower limit (Fleming *et al.*, 1980). A more precise treatment of thermal vibrations, necessitated by this divergence, is to calculate the relative phase of X-rays scattered from two points in the sample a distance  $|\mathbf{r}|$  apart. The appropriate integral that replaces the Debye–Waller integral is

$$\langle [u(\mathbf{r}) - u(0)]^2 \rangle \simeq \frac{k_{\text{B}}T}{c^3} \int \sin^2(\mathbf{k} \cdot \mathbf{r}) \frac{dk}{k} d\{\cos(\mathbf{k} \cdot \mathbf{r})\} \quad (4.4.3.2)$$

#### 4. DIFFUSE SCATTERING AND RELATED TOPICS

and the divergence due to the lower limit is cut off by the fact that  $\sin^2(\mathbf{k} \cdot \mathbf{r})$  vanishes as  $k \rightarrow 0$ . More complete analysis obtains  $\langle [u(\mathbf{r}) - u(0)]^2 \rangle \simeq (k_B T/c^2) \ln(|\mathbf{r}|/a)$ , where  $a \approx$  atomic size. If this is exponentiated, as for the Debye–Waller factor, the density–density correlation function can be shown to have the form  $\langle \rho(\mathbf{r})\rho(0) \rangle \simeq |\mathbf{r}/a|^{-\eta}$ , where  $\eta \simeq |\mathbf{q}|^2(k_B T/c^2)$  and  $|\mathbf{q}| \simeq 2\pi/a$ . In place of the usual periodic density–density correlation function of three-dimensional crystals, the periodic correlations of two-dimensional crystals decay as some power of the distance. This type of positional order, in which the correlations decay as some power of the distance, is the quasi-long-range order (QLRO) that appears in Tables 4.4.1.1 and 4.4.1.2. It is distinguished from true long-range order (LRO) where the correlations continue indefinitely, and short-range order (SRO) where the positional correlations decay exponentially as in either a simple fluid or a nematic liquid crystal.

The usual prediction of Bragg scattering for three-dimensional crystals is obtained from the Fourier transform of the three-dimensional density–density correlation function. Since the correlation function is made up of periodic and random parts, it follows that the scattering cross section is made up of a  $\delta$  function at the Bragg condition superposed on a background of thermal diffuse scattering from the random part. In principle, these two types of scattering can be separated empirically by using a high-resolution spectrometer that integrates all of the  $\delta$ -function Bragg peak, but only a small part of the thermal diffuse scattering. Since the two-dimensional lattice is not strictly periodic, there is no formal way to separate the periodic and random parts, and the Fourier transform for the algebraic correlation function obtains a cross section that is described by an algebraic singularity of the form  $|\mathbf{Q} - \mathbf{q}|^{\eta-2}$  (Gunther *et al.*, 1980). In 1972, Caillé (Caillé, 1972) presented an argument that the X-ray scattering line shape for the one-dimensional periodicity of the smectic-A system in three dimensions has an algebraic singularity that is analogous to the line shapes from two-dimensional crystals.

In three-dimensional crystals, both the longitudinal and the shear sound waves satisfy linear dispersion relations of the form  $\omega = ck$ . In simple liquids, and also for nematic liquid crystals, only the longitudinal sound wave has such a linear dispersion relation. Shear sound waves are overdamped and the decay rate  $1/\tau$  is given by the imaginary part of a dispersion relation of the form  $\omega = i(\eta/\rho)k^2$ , where  $\eta$  is a viscosity coefficient and  $\rho$  is the liquid density. The intermediate order of the smectic-A mesomorphic phase, between the three-dimensional crystal and the nematic, results in one of the modes for shear sound waves having the curious dispersion relation  $\omega^2 = c^2 k_\perp^2 k_z^2 / (k_\perp^2 + k_z^2)$ , where  $k_\perp$  and  $k_z$  are the magnitudes of the components of the acoustic wavevector perpendicular and parallel to  $\langle \mathbf{n} \rangle$ , respectively (De Gennes, 1969*a*; Martin *et al.*, 1972). More detailed analysis, including terms of higher order in  $k_\perp^2$ , obtains the equivalent of the Debye–Waller factor for the smectic-A as

$$W \simeq k_B T \int_0^{k_D} \frac{k_\perp dk_\perp dk_z}{Bk_z^2 + Kk_\perp^4}, \quad (4.4.3.3)$$

where  $B$  and  $K$  are smectic elastic constants,  $k_\perp^2 = k_x^2 + k_y^2$ , and  $k_D$  is the Debye wavevector. On substitution of  $u^2 = (K/B)k_\perp^2 + k_z^2$ , the integral can be manipulated into the form  $\int du/u$ , which diverges logarithmically at the lower limit in exactly the same way as the integral for the Debye–Waller factor of the two-dimensional crystal. The result is that the smectic-A phase has a sharp peak, described by an algebraic cusp, at the place in reciprocal space where one would expect a true  $\delta$ -function Bragg cross section from a truly periodic one-dimensional lattice. In fact, the lattice is not truly periodic and the smectic-A system has only QLRO along the direction  $\langle \mathbf{n} \rangle$ .

X-ray scattering experiments to test this idea were carried out on one thermotropic smectic-A system, but the results, while consistent with the theory, were not adequate to provide an unambiguous proof of the algebraic cusp (Als-Nielsen *et al.*, 1980). One of the principal difficulties was due to the fact that, when thermotropic samples are oriented in an external magnetic field in the higher-temperature nematic phase and then gradually cooled through the nematic to smectic-A phase transition, the smectic-A samples usually have mosaic spreads of the order of a fraction of a degree and this is not sufficient for detailed line-shape studies near to the peak. A second difficulty is that, in most of the thermotropic smectic-A phases that have been studied to date, only the lowest-order peak is observed. It is not clear whether this is due to a large Debye–Waller-type effect or whether the form factor for the smectic-A layer falls off this rapidly. Nevertheless, since the factor  $\eta$  in the exponent of the cusp  $|\mathbf{Q} - \mathbf{q}|^{\eta-2}$  depends quadratically on the magnitude of the reciprocal vector  $|\mathbf{q}|$ , the shape of the cusp for the different orders would constitute a severe test of the theory.

Fortunately, it is common to observe multiple orders for lyotropic smectic-A systems and such an experiment, carried out on the lyotropic smectic-A system formed from a quaternary mixture of sodium dodecyl sulfate, pentanol, water and dodecane, confirmed the theoretical predictions for the Landau–Peierls effect in the smectic-A phase (Safinya, Roux *et al.*, 1986). The problem of sample mosaic was resolved by using a three-dimensional powder. Although the conditions on the analysis are delicate, Safinya *et al.* demonstrated that for a perfect powder, for which the microcrystals are sufficiently large, the powder line shape does allow unambiguous determination of all of the parameters of the anisotropic line shape.

The only other X-ray study of a critical property on the smectic-A side of the transition has been a measurement of the temperature dependence of the integrated intensity of the peak. For three-dimensional crystals, the integrated intensity of a Bragg peak can be measured for samples with poor mosaic distributions, and because the differences between QLRO and true LRO are only manifest at long distances in real space, or at small wavevectors in reciprocal space, the same is true for the ‘quasi-Bragg peak’ of the smectic-A phase. Chan *et al.* measured the temperature dependence of the integrated intensity of the smectic-A peak across the nematic to smectic-A phase transition for a number of liquid crystals with varying exponents  $\nu_\parallel$  and  $\nu_\perp$  (Chan, Deutsch *et al.*, 1985). For the Landau–De Gennes free-energy density (equation 4.4.2.5), the theoretical prediction is that the critical part of the integrated intensity should vary as  $|t|^x$ , where  $x = 1 - \alpha$  when the critical part of the heat capacity diverges according to the power law  $|t|^{-\alpha}$ . Six samples were measured with values of  $\alpha$  varying from 0 to 0.5. Although for samples with  $\alpha \approx 0.5$  the critical intensity did vary as  $x \approx 0.5$ , there were systematic deviations for smaller values of  $\alpha$ , and for  $\alpha \approx 0$  the measured values of  $x$  were in the range 0.7 to 0.76. The origin of this discrepancy is not at present understood.

Similar integrated intensity measurements in the vicinity of the first-order nematic to smectic-C transition cannot easily be made in smectic-C samples since the magnetic field aligns the molecular axis  $\langle \mathbf{n} \rangle$ , and when the layers form at some angle  $\varphi$  to  $\langle \mathbf{n} \rangle$  the layer normals are distributed along the full  $2\pi$  of azimuthal directions around  $\langle \mathbf{n} \rangle$ , as shown in Fig. 4.4.1.2(d). The X-ray scattering pattern for such a sample is a partial powder with a peak-intensity distribution that forms a ring of radius  $|\mathbf{q}| \sin(\varphi)$ . The opening of the single spot along the average molecular axis  $\langle \mathbf{n} \rangle$  into a ring can be used to study either the nematic to smectic-C or the smectic-A to smectic-C transition (Martinez-Miranda *et al.*, 1986).

The statistical physics in the region of the phase diagram surrounding the triple point, where the nematic, smectic-A and smectic-C phases meet, has been the subject of considerable theoretical speculation (Chen & Lubensky, 1976; Chu &

#### 4.4. SCATTERING FROM MESOMORPHIC STRUCTURES

McMillan, 1977; Benguigui, 1979; Huang & Lien, 1981; Grinstein & Toner, 1983). The best representation of the observed X-ray scattering structure near the nematic to smectic-A, the nematic to smectic-C and the nematic/smectic-A/smectic-C (NAC) multicritical point is obtained from the mean-field theory of Chen and Lubensky, the essence of which is expressed in terms of an energy density of the form

$$\Delta F(\psi) = \frac{A}{2} |\psi|^2 + \frac{D}{4} |\psi|^4 + \frac{1}{2} [E_{\parallel} (Q_{\parallel}^2 - Q_0^2) + E_{\perp} Q_{\perp}^2 + E_{\perp\perp} Q_{\perp}^4 + E_{\perp\parallel} Q_{\perp}^2 (Q_{\parallel}^2 - Q_0^2)] |\psi(\mathbf{Q})|^2, \quad (4.4.3.4)$$

where  $\psi = \psi(\mathbf{Q})$  is the Fourier component of the electron density:

$$\psi(\mathbf{Q}) \equiv \frac{1}{(2\pi)^3} \int d^3\mathbf{r} \exp[i(\mathbf{Q} \cdot \mathbf{r})] \rho(\mathbf{r}). \quad (4.4.3.5)$$

The quantities  $E_{\parallel}$ ,  $E_{\perp\perp}$ , and  $E_{\perp\parallel}$  are all positive definite; however, the sign of  $A$  and  $E_{\perp}$  depends on temperature. For  $A > 0$  and  $E_{\perp} > 0$ , the free energy, including the higher-order terms, is minimized by  $\psi(\mathbf{Q}) = 0$  and the nematic is the stable phase. For  $A < 0$  and  $E_{\perp} > 0$ , the minimum in the free energy occurs for a nonvanishing value for  $\psi(\mathbf{Q})$  in the vicinity of  $Q_{\parallel} \approx Q_0$ , corresponding to the uniaxial smectic-A phase; however, for  $E_{\perp} < 0$ , the free-energy minimum occurs for a nonvanishing  $\psi(\mathbf{Q})$  with a finite value of  $Q_{\perp}$ , corresponding to smectic-C order. The special point in the phase diagram where two terms in the free energy vanish simultaneously is known as a 'Lifshitz point' (Hornreich *et al.*, 1975). In the present problem, this occurs at the triple point where the nematic, smectic-A and smectic-C phases coexist. Although there have been other theoretical models for this transition, the best agreement between the observed and theoretical line shapes for the X-ray scattering cross sections is based on the Chen-Lubensky model. Most of the results from light-scattering experiments in the vicinity of the NAC triple point also agree with the main features predicted by the Chen-Lubensky model; however, there are some discrepancies that are not explained (Solomon & Litster, 1986).

The nematic to smectic-C transition in the vicinity of this point is particularly interesting in that, on approaching the nematic to smectic-C transition temperature from the nematic phase, the X-ray scattering line shapes first appear to be identical to the shapes usually observed on approaching the nematic to smectic-A phase transition; however, within approximately 0.1 K of the transition, they change to shapes that clearly indicate smectic-C-type fluctuations. Details of this crossover are among the strongest evidence supporting the Lifshitz idea behind the Chen-Lubensky model.

##### 4.4.3.2. Modulated smectic-A and smectic-C phases

Previously, we mentioned that, although the reciprocal-lattice spacing  $|\mathbf{q}|$  for many smectic-A phases corresponds to  $2\pi/L$ , where  $L$  is the molecular length, there are a number of others for which  $|\mathbf{q}|$  is between  $\pi/L$  and  $2\pi/L$  (Leadbetter, Frost, Gaughan, Gray & Mosley, 1979; Leadbetter *et al.*, 1977). This suggests the possibility of different types of smectic-A phases in which the bare molecular length is not the sole determining factor of the period  $d$ . In 1979, workers at Bordeaux optically observed some sort of phase transition between two phases that both appeared to be of the smectic-A type (Sigaud *et al.*, 1979). Subsequent X-ray studies indicated that in the nematic phase these materials simultaneously displayed critical fluctuations with two separate periods (Levelut *et al.*, 1981; Hardouin *et al.*, 1980, 1983; Ratna *et al.*, 1985, 1986; Chan, Pershan *et al.*, 1985, 1986; Safinya, Varady *et al.*, 1986; Fontes *et al.*, 1986) and confirmed phase transitions

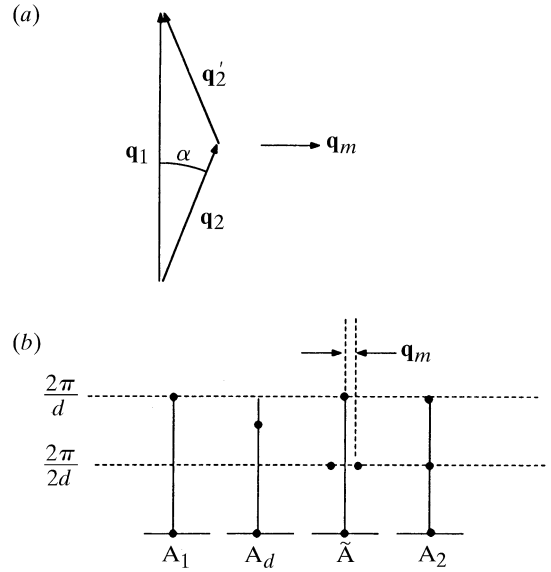


Fig. 4.4.3.1. (a) Schematic illustration of the necessary condition for coupling between order parameters when  $|\mathbf{q}_2| < 2|\mathbf{q}_1|$ ;  $|\mathbf{q}| = (|\mathbf{q}_2|^2 - |\mathbf{q}_1|^2)^{1/2} = |\mathbf{q}_1| \sin(\alpha)$ . (b) Positions of the principal peaks for the indicated smectic-A phases.

between phases that have been designated smectic-A<sub>1</sub> with period  $d \approx L$ , smectic-A<sub>2</sub> with period  $d \approx 2L$  and smectic-A<sub>d</sub> with period  $L < d < 2L$ . Stimulated by the experimental results, Prost and co-workers generalized the De Gennes mean-field theory by writing

$$\rho(\mathbf{r}) = \langle \rho \rangle + \text{Re}\{\Psi_1 \exp(i\mathbf{q}_1 \cdot \mathbf{r}) + \Psi_2 \exp(i\mathbf{q}_2 \cdot \mathbf{r})\},$$

where 1 and 2 refer to two different density waves (Prost, 1979; Prost & Barois, 1983; Barois *et al.*, 1985). In the special case that  $\mathbf{q}_1 \approx 2\mathbf{q}_2$  the free energy represented by equation (4.4.2.3) must be generalized to include terms like

$$(\Psi_2^*)^2 \Psi_1 \exp[i(\mathbf{q}_1 - 2\mathbf{q}_2) \cdot \mathbf{r}] + \text{c.c.}$$

that couple the two order parameters. Suitable choices for the relative values of the phenomenological parameters of the free energy then result in minima that correspond to any one of these three smectic-A phases. Much more interesting, however, was the observation that even if  $|\mathbf{q}_1| < 2|\mathbf{q}_2|$  the two order parameters could still be coupled together if  $\mathbf{q}_1$  and  $\mathbf{q}_2$  were not collinear, as illustrated in Fig. 4.4.3.1(a), such that  $2\mathbf{q}_1 \cdot \mathbf{q}_2 = |\mathbf{q}_1|^2$ . Prost *et al.* predicted the existence of phases that are modulated in the direction perpendicular to the average layer normal with a period  $4\pi/[|\mathbf{q}_2| \sin(\varphi)] = 2\pi/|\mathbf{q}_m|$ . Such a modulated phase has been observed and is designated as the smectic-A (Hardouin *et al.*, 1981). Similar considerations apply to the smectic-C phases and the modulated phase is designated smectic-C̃; (Hardouin *et al.*, 1982; Huang *et al.*, 1984; Safinya, Varady *et al.*, 1986).

##### 4.4.3.3. Surface effects

The effects of surfaces in inducing macroscopic alignment of mesomorphic phases have been important both for technological applications and for basic research (Sprokel, 1980; Gray & Goodby, 1984). Although there are a variety of experimental techniques that are sensitive to mesomorphic surface order (Beaglehole, 1982; Faetti & Palleschi, 1984; Faetti *et al.*, 1985; Gannon & Faber, 1978; Miyano, 1979; Mada & Kobayashi, 1981; Guyot-Sionnest *et al.*, 1986), it is only recently that X-ray scattering techniques have been applied to this problem. In one form or another, all of the techniques for obtaining surface specificity

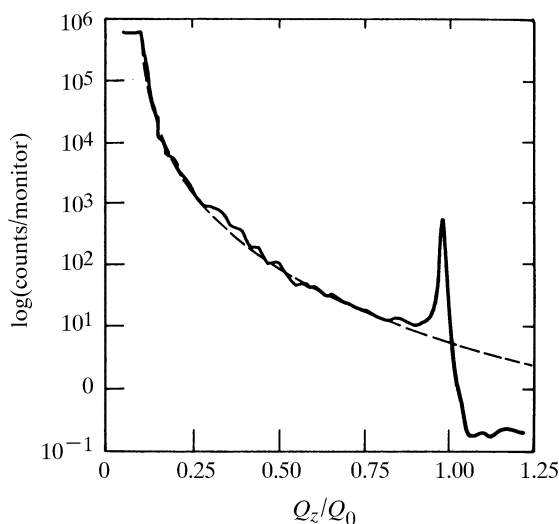


Fig. 4.4.3.2. Specular reflectivity of  $\sim 8$  keV X-rays from the air-liquid interface of the nematic liquid crystal 8OCB 0.05 K above the nematic to smectic-A transition temperature. The dashed line is the Fresnel reflection law as described in the text.

in an X-ray measurement make use of the fact that the average interaction between X-rays and materials can be treated by the introduction of a dielectric constant  $\varepsilon \approx 1 - (4\pi\rho e^2/m\omega^2) = 1 - \rho r_e \lambda^2/\pi$ , where  $\rho$  is the electron density,  $r_e$  is the classical radius of the electron, and  $\omega$  and  $\lambda$  are the angular frequency and the wavelength of the X-ray. Since  $\varepsilon < 1$ , X-rays that are incident at a small angle to the surface  $\theta_0$  will be refracted in the material toward a smaller angle  $\theta_T \approx (\theta_0^2 - \theta_c^2)^{1/2}$ , where the ‘critical angle’  $\theta_c \approx (\rho r_e \lambda^2/\pi)^{1/2} \approx 0.003$  rad ( $\approx 0.2^\circ$ ) for most liquid crystals (Warren, 1968). Although this is a small angle, it is at least two orders of magnitude larger than the practical angular resolution available in modern X-ray spectrometers (Als-Nielsen *et al.*, 1982; Pershan & Als-Nielsen, 1984; Pershan *et al.*, 1987). One can demonstrate that for many conditions the specular reflection  $R(\theta_0)$  is given by

$$R(\theta_0) \approx R_F(\theta_0) |\rho^{-1} \int dz \exp(-iQz) \langle \partial\rho/\partial z \rangle|^2,$$

where  $Q \equiv (4\pi/\lambda) \sin(\theta_0)$ ,  $\langle \partial\rho/\partial z \rangle$  is the normal derivative of the electron density averaged over a region in the surface that is defined by the coherence area of the incident X-ray, and

$$R_F(\theta_0) \approx \left( \frac{\theta_0 - \sqrt{\theta_0^2 - \theta_c^2}}{\theta_0 + \sqrt{\theta_0^2 - \theta_c^2}} \right)^2$$

is the Fresnel reflection law that is calculated from classical optics for a flat interface between the vacuum and a material of dielectric constraint  $\varepsilon$ . Since the condition for specular reflection, that the incident and scattered angles are equal and in the same plane, requires that the scattering vector  $\mathbf{Q} = \hat{z}(4\pi/\lambda) \sin(\theta_0)$  be parallel to the surface normal, it is quite practical to obtain, for flat surfaces, an unambiguous separation of the specular reflection signal from all other scattering events.

Fig. 4.4.3.2(a) illustrates the specular reflectivity from the free nematic-air interface for the liquid crystal 4'-octyloxybiphenyl-4-carbonitrile (8OCB) 0.050 K above the nematic to smectic-A phase-transition temperature (Pershan & Als-Nielsen, 1984). The dashed line is the Fresnel reflection  $R_F(\theta_0)$  in units of  $\sin(\theta_0)/\sin(\theta_c)$ , where the peak at  $\theta_c = 1.39^\circ$  corresponds to surface-induced smectic order in the nematic phase: *i.e.* the selection rule for specular reflection has been used to separate the specular reflection from the critical scattering from the bulk.

Since the full width at half maximum is exactly equal to the reciprocal of the correlation length for critical fluctuations in the bulk,  $2/\xi_{\parallel}$  at all temperatures from  $T - T_{NA} \approx 0.006$  K up to values near to the nematic to isotropic transition,  $T - T_{NA} \approx 3.0$  K, it is clear this is an example where the gravitationally induced long-range order in the surface position has induced mesomorphic order that has long-range correlations parallel to the surface. Along the surface normal, the correlations have only the same finite range as the bulk critical fluctuations. Studies on a number of other nematic (Gransbergen *et al.*, 1986; Ocko *et al.*, 1987) and isotropic surfaces (Ocko, Braslau *et al.*, 1986) indicate features that are specific to local structure of the surface.

#### 4.4.4. Phases with in-plane order

Although the combination of optical microscopy and X-ray scattering studies on unoriented samples identified most of the mesomorphic phases, there remain a number of subtle features that were only discovered by spectra from well oriented samples (see the extensive references contained in Gray & Goodby, 1984). Nematic phases are sufficiently fluid that they are easily oriented by either external electric or magnetic fields, or surface boundary conditions, but similar alignment techniques are not generally successful for the more ordered phases because the combination of strains induced by thermal expansion and the enhanced elasticity that accompanies the order creates defects that do not easily anneal. Other defects that might have been formed during initial growth of the phase also become trapped and it is difficult to obtain well oriented samples by cooling from a higher-temperature aligned phase. Nevertheless, in some cases it has been possible to obtain crystalline-B samples with mosaic spreads of the order of a fraction of a degree by slowing cooling samples that were aligned in the nematic phase. In other cases, mesomorphic phases were obtained by heating and melting single crystals that were grown from solution (Benattar *et al.*, 1979; Leadbetter, Mazid & Malik, 1980).

Moncton & Pindak (1979) were the first to realize that X-ray scattering studies could be carried out on the freely suspended films that Friedel (1922) described in his classical treatise on liquid crystals. These samples, formed across a plane aperture (*i.e.* approximately 1 cm in diameter) in the same manner as soap bubbles, have mosaic spreads that are an order of magnitude smaller. The geometry is illustrated in Fig. 4.4.4.1(a). The substrate in which the aperture is cut can be glass (*e.g.* a microscope cover slip), steel or copper sheeting *etc.* A small amount of the material, usually in the high-temperature region of the smectic-A phase, is spread around the outside of an aperture that is maintained at the necessary temperature, and a wiper is used to drag some of the material across the aperture. If a stable film is successfully drawn, it is detected optically by its finite reflectivity. In particular, against a dark background and with the proper illumination it is quite easy to detect the thinnest free films.

In contrast to conventional soap films that are stabilized by electrostatic effects, smectic films are stabilized by their own layer structure. Films as thin as two molecular layers can be drawn and studied for weeks (Young *et al.*, 1978). Thicker films of the order of thousands of layers can also be made and, with some experience in depositing the raw material around the aperture and the speed of drawing, it is possible to draw films of almost any desired thickness (Moncton *et al.*, 1982). For films thinner than approximately 20 to 30 molecular layers (*i.e.* 600 to 1000 Å), the thickness is determined from the reflected intensity of a small helium-neon laser. Since the reflected intensities for films of 2, 3, 4, 5, ... layers are in the ratio of 4, 9, 16, 25, ..., the measurement can be calibrated by drawing and measuring a reasonable number of thin films. The most straightforward method for thick films is to measure the ellipticity of the polarization induced in laser light transmitted through the film at an